Intra- and Intermolecular Electrial Effects on Nuclear Magnetic Resonance, Nuclear Quadrupole Resonance and Infra-Red pectroscopic Parameters from Ab Initio Calculation and Experiment: From CO to Proteins

Joseph D. Augspurger and Clifford E. Dykstra
Department of Chemistry
Indiana University-Purdue University at Indianapolis
1125 East 38th Street
Indianapolis, IN 46205, USA

Eric Oldfield and John G. Pearson
Department of Chemistry
University of Illinois at Urbana-Champaign
505 South Mathews Avenue
Urbana, IL 61801, USA

ABSTRACT. We examine the role of electrostatic influences on chemical shifts, quadrupole couplings, and vibrational frequencies in proteins as well as small prototype molecules. The goal is to test the notion that the primary change in electronic structure is that of electrical polarization. It is shown that the effects of these interactions on molecular properties are accurately determined by properties which can be calculated by analytical differentiation at the SCF level with Derivative Hartree-Fock (DHF) theory. Several applications of this model are compared with experiment.

Introduction

In this paper, we discuss progress towards obtaining a better understanding of the origins of chemical shifts and infra-red vibrational frequencies in proteins. The origins of the chemical shift nonequivalences due to folding a protein (or nucleic acid) into its native conformation are poorly understood, a somewhat surprising situation given the central importance of folding-induced shielding changes in permitting application of multi-dimensional NMR studies of protein structure (1). Early workers noted in ^{1}H NMR that a number of residues in e.g. hen egg white lysozyme (EC 3.2.1.17) could be resolved (2), and in 1973, Allerhand et al. (3) observed very large chemical shift non-equivalences, due to folding, in the ^{13}C NMR spectra of lysozyme. For C$^{\gamma}$ of the six Trp residues, folding produced a ~ 6 ppm range of chemical shifts, which was almost completely removed upon protein denaturation (3).

Other workers have also observed very large chemical shift ranges for other nuclei in proteins, about 12 ppm for ^{19}F (4-6) and up to ~25 ppm for ^{15}N (7). Similarly, we have observed about a 10 ppm chemical shift range for ^{17}O in C^{17}O labelled heme proteins(8), and very recently, we have observed an unprecedented 15 ppm chemical shift range for

J. A. Tossell (ed.), Nuclear Magnetic Shieldings and Molecular Structure, 75–94.

fluorotryptophan-labelled hen egg white lysozyme (17 ppm in the presence of the inhibitor $(NAG)_3$), due almost entirely due to folding (9).

Given the increasing body of chemical shift data becoming available on proteins, there has been a renewed interest in interpreting the chemical shift changes caused by folding, with most emphasis being placed on the ^1H nucleus (10-21). One general conclusion of these studies is that CH^α proton resonances are shifted downfield in β-sheet regions, while upfield shifts (from the random coil values) are seen for α-helices. All of these investigations have employed empirical correlations between shielding and some structural parameter, and many interesting observations have been made. Of particular utility is the "digital" (or tri-state) approach of Wishart et al. (21) to predicting secondary structure, in which observed shifts are assigned, based on their relationship to the random coil shift, a "-1", "0", or "1" index, corresponding to helix, (random) coil or sheet structure. Applying some simple rules, excellent correlations with known secondary structure were observed. However, the *origins* of these shielding effects have not yet been fully explained. For ^1H NMR, although very large data bases are available, there are many contributions to the observed shielding, including:

- ring current effects
- magnetic susceptibility anisotropies (principally of peptide CO groups)
- electric field effects (helix dipoles, fixed charges, "hydrogen bonding", etc.)

Several groups have used multi-parameter optimization methods in which initial estimates of the electric (E) and magnetic (B) field shifts are iterated to give a best fit with experiment, but there are uncertainities associated with this approach. 10 or 11 parameters need to be optimized, using even semi-classical approaches, which do not include **electronic** structural changes due to helix/sheet conformations, and in addition, there are many possible **models** for the E-field effects - uniform fields, $(field)^2$ terms, field gradients, etc. (22,23). Similar empirical correlations between secondary structure and chemical shielding have also recently been reported for $^{13}C^\alpha$ (24), but a detailed quantum chemical analysis of these shieldings has not yet been reported. Moreover, the empirical approaches have been much less successful for e.g. NH protons, and for ^{15}N or ^{19}F, essentially no predictions have yet been made, even though the chemical shift ranges are ≈15-25 ppm. Thus, more rigorous approaches to the shielding of the heavier elements, as well as hydrogen, need to be developed.

The focus of our current work is to develop models of long range effects upon chemical shielding, due to **electrostatic** fields, using a combination of quantum chemical, molecular dynamics and electrostatics calculations. To date, only simple electrostatic (Coulomb) models have been employed for H^α and HN, and we believe that more realistic modelling of the effects of electric fields should lead to better agreement with experiment - especially for ^{13}C, ^{15}N and ^{19}F. As we describe below, the effects of fields, field gradients and $(field)^2$ terms may all need to be investigated, combined with energy minimization/molecular dynamics methods, using a variety of force fields, and electrostatic modelling methods. We suggest below that long range, weak electrical interactions are large for the heavier elements, and these weak interactions may influence infra-red vibrational frequencies (as well as pure quadrupole frequencies).

Calculation of NMR Parameters by Ab Initio Methods

The first aspect of our efforts to develop models for shielding is the direct ab initio calculation of shielding and related properties for small prototype molecules. Numerous

molecular properties are derivatives of the energy of the molecular eigenstate. For example, the dipole polarizability is the second derivative with respect to the strength of an applied electric field. Magnetic susceptibilities, harmonic vibrational frequencies, and chemical shielding tensors are still other examples of properties that are formally defined as second energy derivatives. Hyperpolarizabilities, hypersusceptibilities and so on, are still higher order derivatives. The analytical evaluation of these energy derivatives follows from differentiating the Schrödinger equation and solving the resulting equations, which are generally inhomogeneous differential equations. If energy and wavefunction in the presence of a perturbation are expressed as Taylor series, then the coefficients of the series are the derivatives. Explicit, recursive expressions for these derivatives are given as well by Rayleigh-Schrödinger perturbation theory (RSPT) (25), and it is possible, in principle, to organize the solutions of the RSPT inhomogeneous equations in an open-ended manner. Alternatively, derivative quantities may be obtained by finite differences, but usually an analytical procedure is preferred because of the possible numerical errors in finite difference procedures and/or the substantial number of differences required for higher order property values.

A direct differentiation approach can be applied to the Hartree-Fock equation to evaluate derivatives (and therefore properties) of the SCF energy (26-29). One approach to analytic differentiation, derivative Hartree-Fock (DHF) theory, has been developed (30,31) to be completely open-ended with respect to both the number of parameters and the order of differentiation. It is general with respect to real or imaginary perturbations, and whether the basis is perturbation dependent (e.g. geometrical derivatives) or not. It has the further advantage of a fully implemented 2N/2N+1 energy derivative evaluation, where only Nth order derivatives of the wavefunction are required to calculate 2N and 2N+1 order energy derivatives. Since the wavefunction derivatives are the computationally intensive step, this enhances computational efficiency. DHF requires as input the SCF wavefunction coefficient matrix, the one- and two- electron operator integrals, integrals over derivatives of the hamiltonian, and in the case of basis dependent perturbations derivatives of the one- and two- electron integrals. We have developed associated algorithms for readily obtaining all such integrals (32,33).

The chemical shielding of a particular nucleus is formally defined as the second derivative of the energy with respect to the strength of a uniform external magnetic field and the magnetic dipole moment of the nucleus. A particular element of the chemical shielding tensor is

$$\sigma_{\alpha\beta} = \frac{\partial^2 E}{\partial \mu_\alpha \partial B_\beta} \qquad (1)$$

These elements can be calculated at the SCF level with DHF. But in addition, there are higher order properties which are relevant to our ultimate goal. To consider the effects of an external electric field on the chemical shift, $\sigma_{\alpha\beta}$, one can first consider the derivative of $\sigma_{\alpha\beta}$ with respect to the electric field strength, a third derivative property designated A:

$$A_{\alpha\beta,\gamma} = \frac{\partial \sigma_{\alpha\beta}}{\partial V_\gamma} = \frac{\partial^3 E}{\partial \mu_\alpha \partial B_\beta \partial V_\gamma} \qquad (2)$$

We may term the quantity $A_{\alpha\beta,\gamma}$ a dipole shielding polarizability, as it is the first derivative of the chemical shielding with respect to an external electric field, analogous to the dipole polarizability being the first derivative of the dipole moment with respect to an electric field. Extending the terminology, the dipole shielding hyperpolarizability, B, is the second derivative of the shielding with respect to the electric field, which is a fourth derivative property. The effects of non-uniform fields can be examined as well by differentiating with respect to a field gradient to calculate the quadrupole shielding polarizability, C, and so on.

In calculating these electro-magnetic properties, basis set completeness is perhaps the foremost concern. One would like to use the smallest basis which achieves the desired accuracy in determining molecular structures or properties. Often, practical considerations (computation time, memory, disk space, etc.) place constraints on the basis size. One means of evaluating completeness is to systematically enlarge bases and test the property for convergence with respect to further basis enlargement. When incorporating the effects of an external magnetic field on a molecule, the additional issue of gauge dependence arises (27). With a complete basis, any magnetic property, such as magnetic susceptibility or chemical shielding, is invariant to the choice of gauge. With a truncated basis, this invariance may not result, and so gauge invariance sometimes is taken as another criterion for judging basis completeness.

In practice, the choice of gauge is often that which appears to lead to the most correct property values for a truncated basis. The center of charge, the center of mass, or a nuclear center have been common choices. Chan and Das (34) showed that choosing the electronic centroid of charge minimized the paramagnetic susceptibility. Ditchfield (35) developed an approach to Hartree-Fock perturbation theory using gauge invariant atomic orbitals (GIAO). These incorporate the magnetic vector potential into the basis functions. However, it is the properties which are invariant, and so this type of basis is better described as gauge-dependent (36). Epstein (37) subsequently demonstrated that the resultant GIAO wavefunction is not invariant to gauge transformation, even though the energy is. He termed this "enforced gauge invariance" for it results not from basis completeness, but from the basis always being returned to the original gauge by the built-in dependence on the magnetic vector potential. Sadlej (38) proposed a criterion for choosing the gauge origin which minimizes the error with respect to gauge origin. This criterion is the quantity $[\langle 0|A(R)B(R)|0\rangle - \sum_K \langle 0|A(R)|K\rangle\langle K|B(R)|0\rangle]$, where $|0\rangle$ is the ground state SCF wavefunction, $|K\rangle$ the other Slater determinants which arise from the SCF orbitals, and where A and B are operators which depend on the gauge origin. A similar proposal was made by Yaris (39). Kutzelnigg and Schindler have introduced an approach where an individual gauge for each localized orbital (IGLO) is used in incorporating dependence on the vector potential into the basis so that molecular properties can be built up from atomic and bond contributions (40,41). Hansen and Bouman (42) have applied a conceptually similar local orbital/local origin (LORG) approach. Lazzeretti et. al. (43-45) have likewise introduced a multiple-origin gauge method, this one based on computing susceptibilities from nuclear electric shieldings which they term "distributed origin gauge with origin at the nuclei (DOGON)" (45). Geertsen (46,47) has shown that a polarization propagator based method leads to gauge invariant susceptibilities for limited basis sets. Hinton and Pulay have recently found means for improving the efficiency of GIAO calculations (48, 49). In many ways, these are attempts to achieve proper results from conventional-sized bases versus extended bases. We may also examine the issue of basis set completeness vis-a-vis gauge sensitivity through very extended bases, and in particular to look at a wider class of

properties, magneto-electrical response properties. Gauge sensitivity for these properties has been considered rarely, perhaps the earliest case being the calculations of Day and Buckingham on hydrogen fluoride (50).

There have been quite a number of important studies of basis set requirements for accurate calculation of purely magnetic second order properties, e.g. susceptibilities and chemical shieldings. Lazzeretti, et al. (51,52) examined several small molecules, using basis sets that ranged from minimal up to better than triple zeta, doubly polarized. Kutzelnigg and Schindler (41) carried out similar tests using the IGLO method with similar bases, and also went beyond to include triply polarized sets, with a single 4f function on first row atoms. More recently, Chesnut has conducted tests of small basis sets using Ditchfield's GIAO approach (35) for calculating the chemical shieldings of small molecules of first row atoms (53), larger basis calculations for molecules of second row atoms (54), and use of locally dense basis sets (55), where the nucleus for which the shielding is to be calculated has a larger basis set than other atoms in the molecule. We may expect that the basis set requirements to be somewhat similar for magneto-electric properties, and our results show to what extent this holds.

We calculated the chemical shielding and the shielding polarizability of carbon monoxide with a number of basis sets at several gauge origins on the molecular axis to evaluate the gauge dependence as a function of basis set size and also to examine the property convergence (56). The valence sets used were Dunning's double zeta (DZ) (9s5p/4s2p) and triple zeta (TZ) (10s6p/6s3p) contractions (57) of Huzinaga's primitive sets (58). An initial finding was that added flexibility in the valence p set had a noticeable effect, and so two other valence sets were constructed by uncontracting the two most

TABLE 1. Exponent Values of the Uncontracted, Diffuse and Polarization Gaussian Functions that Were Used to Augment Double-Zeta and Triple Zeta Sets[a].

Basis Designation[b]	s	p	d	f
DZP/DZ'P			0.75/0.80	
TZP/TZ'P			0.75/0.80	
TZ'2P			0.9	
			0.18	
$TZ^{+}3P^{c}$and	0.05/0.06	0.03 /0.05	0.9	
$TZ'^{+}3P$		0.005/0.007	0.13	
			0.02	
$TZ'^{+}3Pf$	0.05/0.06	0.03 /0.05	0.9	0.4
		0.005/0.007	0.13	
			0.02	

[a]Where the exponents of the augmenting functions differ for carbon and oxygen, it is the carbon function exponent that is given first. The oxygen exponent value follows the "/". If there is one value, then the same exponent was used for both carbon and oxygen centers.

[b]The + superscript designates the addition of two uncontracted diffuse p functions and one uncontracted diffuse s function.

[c]This is the Electrical Properties (ELP) basis described in Ref. 59.

diffuse primitive functions of Dunning's contracted gaussian. These are designated DZ' (9s5p/4s4p) and TZ' (10s6p/6s5p). To these valence sets were added one, two and three sets of polarization functions (in some cases augmented with diffuse valence functions as well), up to the largest basis tested which also included one 4f function. Table 1 describes the diffuse valence and polarization functions which augmented the valence basis sets. In these calculations the C atom was placed at the origin, the center of mass at x=1.218Å, and the O atom at x=2.132Å.

The results for the chemical shielding and shielding polarizability of oxygen are given in Fig. 1:

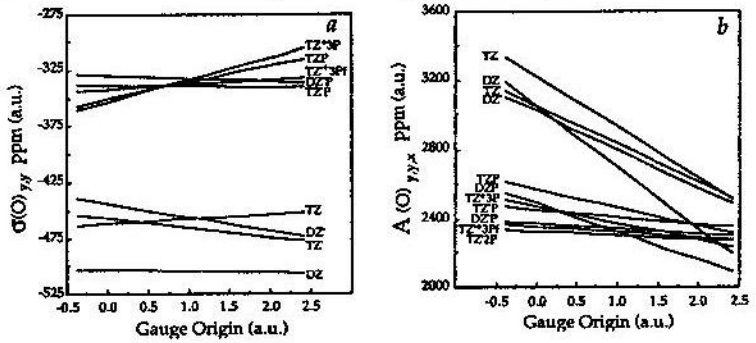

Figure 1. *a)* $\sigma_{y,y}$ and *b)* $A_{yy,x}$ (ppm/a.u.) for ^{17}O as a function of gauge origin along the molecular axis (56). On the scale of the graph for $\sigma_{y,y}$, the DZP basis result is essentially coincident with $TZ^{+}3P$, as are TZ'2P and $TZ'^{+}3P$ with $TZ'^{+}3Pf$. The nearly coincident curves are not displayed. For $A_{yy,x}$, where the $TZ'^{+}3P$ and $TZ'^{+}3Pf$ bases are essentially coincident, only one curve is shown. The carbon atom lies at the origin, the center of mass at 1.218, and the oxygen atom at 2.132.

Since for linear molecules the axial component of the shielding tensor (σ_{xx}) is independent of the gauge origin position on the molecular axis, we concentrated on the off-axis component (σ_{yy}). For the shielding, the unpolarized bases are shown to give results which fall into a group quite separate from the larger bases. It is significant that even the unpolarized bases give shieldings which are quite insensitive to the gauge origin, but which are 100 to 200 ppm lower than the larger basis results. The increased flexibility of TZ versus DZ has a greater effect for the shieldings than for the susceptibility. On the other hand, there is little difference between DZ' and TZ'. Additional polarization functions augmenting the DZ and TZ bases leads to successively less gauge sensitivity (DZP to TZP to $TZ^{+}3P$). For the more flexible DZ' and TZ' bases, adding a single set of polarization functions leads to significant improvement while adding further polarization functions leads to much smaller improvements. There is little difference between the TZ'2P, $TZ'^{+}3P$, and $TZ'^{+}3Pf$ bases. For the ^{17}O shieldings, there is a variance of about 15 ppm over the range of 2.5 a.u. tested, which is a variation of 10 and 5 percent respectively. The results for the shielding polarizabilities show much the same trends.

We also carried out similar tests of the magnetic susceptibility, and the results are given in Fig. 2:

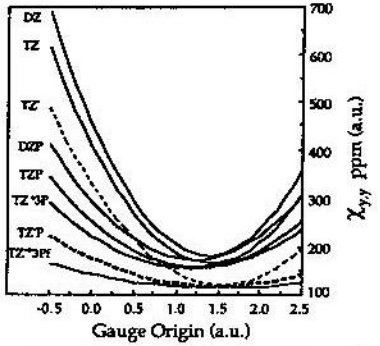

Figure 2. $\chi_{y,y}$ as a function of gauge origin along the molecular axis. On this scale, the DZ' basis results are essentially coincident with the TZ' results, as are those of DZ'P with TZ'P, and of TZ'2P and $TZ'^{+}3P$ with $TZ'^{+}3Pf$; the nearly coincident curves are not displayed. Broken lines are used for clarity only.The carbon atom lies at the origin, the center of mass at 1.218, and the oxygen atom at 2.132.

The susceptibility is evaluated as a derivative similarly to the chemical shielding, only it is the pure second derivative of the energy with respect to the magnetic field.

$$\chi_{\alpha\beta} = \frac{\partial^2 E}{\partial B_\alpha \partial B_\beta} \qquad (3)$$

The most obvious feature of the susceptibility curves is that they exhibit extrema (60), and that basis set enlargement leads fairly smoothly to lessening of gauge dependence. The additional valence flexibility of the TZ valence set versus the DZ valence set leads to a negligible improvement in gauge invariance and a small lowering in the vicinity of the curves' minima. The significant improvement in the valence basis is the de-contraction of the p-set: All DZ' bases are overall better than DZ and TZ' bases are better than TZ. The TZ'P basis shows a marked decrease in gauge dependence over TZ' as evidenced by a flatter curve in Fig. 2. Use of the second set of polarization functions shows a lesser effect, and the additional flexibility of $TZ'^{+}3P$ and $TZ'^{+}3Pf$ shows a continuing but smaller effect.

These results show that basis set tests at a single gauge origin may be misleading: They may suggest convergence when it has not been achieved. Likewise, gauge invariance is not a useful criterion for basis quality; it may be achieved when there is still a considerable error in the property. What seems the best means of assessing the reliability in the range of magneto-electrical properties we have considered is to examine basis set convergence for a range of gauge choices. From the body of results collected here, the TZ'2P basis appears optimal in limiting basis size yet achieving reliable values. Smaller bases such as DZ'P may be appropriate if a slightly larger error is acceptable. Table 2 is a collection of A values for a number of small molecules. These values and higher order

properties have been used to calculate changes in chemical shieldings from external electrical potentials

Table 2. Shielding polarizabilities for several small molecules in ppm/a.u. (31)

Molecule	Nucleus	$\bar{A}_x$ [a]	$\bar{A}_{xx}$ [b]
H_2	H	-50.3	5.8
HCCH	H	-67.2	-109.5
HCN	H	-54.1	89.5
H_2CO	H	0.1	5.0
HF	H	-81.5	61.8
H_2O	H	-47.3	3.5
NH_3	H	-27.7	-18.1
CH_4	H	-45.1	-2.1
SiH_4	H	-35.8	-1.7
H_2CO	C	-697.4	746.0
CO	C	-374.5	532.7
HCN	C	-422.6	512.1
HCCH	C	-733.9	-351.8
CH_4	C	0.0	-54.1
NH_3	N	50.8	333.3
HCN	N	1910.1	603.6
H_2O	O	401.1	-190.8
CO	O	1526.7	1044.0
H_2CO	O	7019.0	1377.8
HF	F	636.5	-741.7
SiH_4	Si	0.0	456.5

[a] $\bar{A}_x = 1/3\,[\,A_{xx,x} + A_{yy,x} + A_{zz,x}\,]$.

[b] $\bar{A}_{xx} = 1/3\,[\,A_{xx,xx} + A_{yy,xx} + A_{zz,xx}\,]$

NMR and IR Results on Proteins

Our ideas about electrical interactions in proteins have developed from recent work on CO-labelled heme proteins, where we observed ^{13}C and ^{17}O chemical shifts for over a dozen proteins, and were also able to determine ^{17}O nuclear quadrupole coupling constants for the bound CO. When we compared each of these three NMR parameters with the CO infra-red vibrational frequency, ν_{CO}, we found excellent correlations between $\delta_i(^{13}C)$, $\delta_i(^{17}O)$, e^2qQ/h (^{17}O) and ν_{CO}, and we explained our results in terms of a weak electrical interaction model (61) in which changes in the vibrational frequency of CO, the ^{13}C and ^{17}O chemical shifts, as well as the ^{17}O nuclear quadrupole coupling constants, were all interpreted as changes due to polarization of CO by large electric fields from the protein. Our model is based on the demonstration by Dykstra that the primary electronic structure change upon weak interaction is electrical polarization (62-64). A typical experimental result showing the relation between ν(C-O) and $\delta_i(^{17}O)$ for CO bound to a number of different heme proteins is shown in Figure 3, and Figure 4 shows

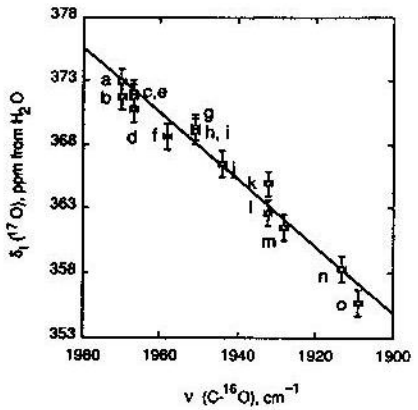

Figure 3. Graph showing relation between (infrared) CO vibrational stretch frequency [ν(C-O), cm^{-1}] and ^{17}O NMR isotropic chemical shift, $\delta_i(^{17}O)$, for heme proteins. Data points for proximal His as well as proximal Cys (chloroperoxidase) containing proteins fall on the same curve. Letters correspond to proteins, as follows: a, *Glycera dibranchiata* hemoglobin; b, synthetic *Physeter catodon* myoglobin His E7 → Val; c, picket fence porphyrin; d, *P. catodon* myoglobin, pH "low"; e, synthetic *P. catodon* myoglobin, His E7 → Phe; f, chloroperoxidase, pH = 6.0; g, rabbit hemoglobin, β chain; h, human adult hemoglobin, α chain; i, human adult hemoglobin, β chain; j, *P. catodon* myoglobin, pH = 7.0; k, horseradish peroxidase isoenzyme C, pH = 10.5; l, horseradish peroxidase isoenzyme A, pH = 9.5; m, rabbit hemoglobin, α chain; n, horseradish peroxidase isoenzyme C, pD = 7.0; o, horseradish isoenzyme A, pD = 4.5.

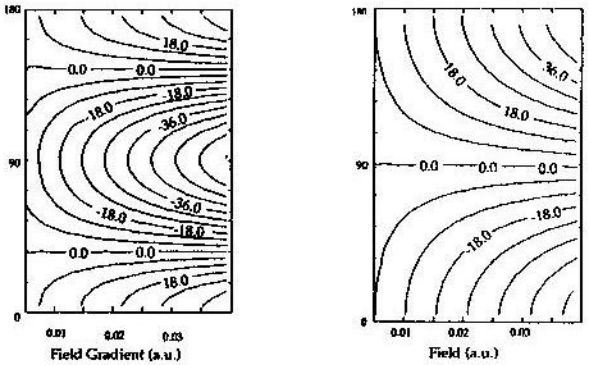

Figure 4. Contours of (a) the isotropic chemical shift at the oxygen nucleus of CO as a function of the strength of an applied field (horizontal axis) and the angle of orientation of the field with respect to the molecular axis (vertical axis), and (b) the isotropic chemical shift at the oxygen nucleus of CO as a function of the strength of an applied field gradient (horizontal axis) and the angle of orientation of the field gradient with respect to the molecular axis (vertical axis) for the ground state of CO.

the perturbation of the ^{17}O chemical shift of free CO due to a uniform field or applied field gradient, obtained by using DHF to calculate the electrical response properties (moments, polarizabilities and hyperpolarizabilities) as well as the chemical shift polarizabilities as a function of the CO separation distance. With these properties, the CO potential energy curve and chemical shift were calculated for a number of different axial electric field/ field gradient strengths, and from these the ground vibrational state chemical shift and fundamental transition frequency calculated. Figure 5a shows the

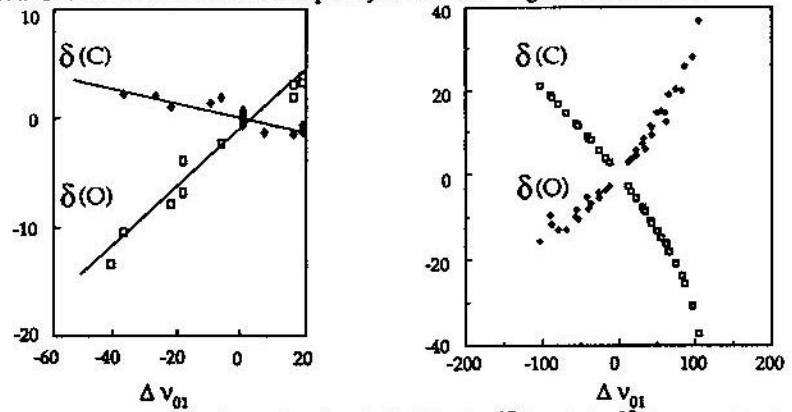

Figure 5. a) Plots of the isotropic chemical shifts for ^{17}O and for ^{13}C versus the change in the fundamental vibrational frequency measured experimentally for a range of carbon monoxyheme proteins; b) Plots of the isotropic chemical shifts for ^{17}O and for ^{13}C versus the change in the fundamental vibrational frequency calculated for various positions of an axial dipole consisting of two point charges.

experimental ^{17}O and ^{13}C chemical shifts of CO bound to heme proteins as a function of CO vibrational frequency (using 1950 cm^{-1} as a nonperturbed zero-frequency reference), while Figure 5b shows the results of DHF calculations of the field and field gradient perturbation of a free CO molecule, again taking the field-free ν_{CO} as a zero reference point.

Although not perfect, the sign and magnitude of the observed NMR and IR frequency shifts are quite well reproduced by the calculation, which tends to support the idea that the uniform component of the fields generated by the protein are responsible for the observed chemical shift changes, and the large (~60 cm^{-1}) range of CO vibrational frequencies. The range of fields required to cause the experimental shifts is ~0.008 au (~$4x10^7$ Vcm^{-1}), a reasonable value for the interior of a protein, where dielectric constants are generally low.

To further test the idea that electrical interactions in proteins make a significant contribution to the observed shieldings, we have computed the $\bar{A}_x$ values for ^1H, ^{13}CO, ^{13}C(aromatic), $C^{17}O$ and ^{19}F in a number of model compounds (see Table II), and compared these $\bar{A}_x$ values with the *observed chemical shielding ranges in proteins*, as shown in the following Figure:

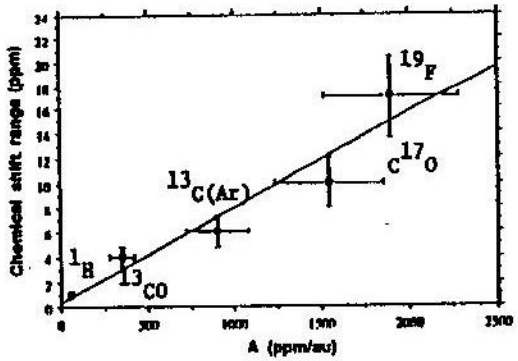

Figure 6. Graph showing relationship between the isotropic dipole shielding polarizabilities computed by using derivative Hartree-Fock theory, and the observed (maximum) chemical shift ranges, for ^1H, ^{13}C, ^{17}O and ^{19}F nuclei in proteins.

All of these results can be fit to a linear equation, assuming the dominance of the dipole shielding polarizability, as:

$$\Delta\delta(\text{ppm}) = 0.00765\ \bar{A}_x + 0.32 \qquad (4)$$

where the slope, ΔV_x, represents the range of effective fields experienced by the nuclei in question. Although Equation (4) is only strictly applicable for highly symmetric systems, the slope we find, $\Delta V_x = 0.00765$ au, appears to be a very reasonable value, based upon previous electrostatic calculations of electric fields in proteins (65). For example, Dao-Ping et al. (65) found an electrostatic field in the active site cleft in lysozymes of up to 13.7 x 10^6 Vcm^{-1} (for an interior dielectric of 4); for ε=2.5 this is 0.0043 au (~$2.2x10^7$ Vcm^{-1}). Thus, the effective range of fields in proteins of ~$3.9x10^7$ Vcm^{-1} determined by this NMR approach is close to the ~$4x10^7$ Vcm^{-1} value we deduced previously from our IR and NMR results (61) and the work of others. However, these fields cannot always be expected to be very uniform, and further work is underway on calculating the non-uniform field contributions to shielding in several systems.

Given these results, it is clear that the next step is to try to interpret individual, assigned chemical shifts in proteins. This is expected to be a lengthy process, since questions about solution-crystal structural differences, dynamical averaging, non-uniform field contributions, and of course, protein electrostatics, all come into play. Nevertheless, preliminary results using a variety of electrostatics models show promise for analyzing the ^{19}F NMR spectra of the *Escherichia coli* galactose binding protein, as shown in Figure 7. Fluorine should be a particularly sensitive probe of protein electrostatics, since its dipole shielding polarizability, $\bar{A}_x$ = 1885 ppm/au (in fluorobenzene) is the largest we have encountered for any of the lighter elements.

Using a simple Coulomb point-charge model, and an energy minimized (500 steps using Biosym Technologies Discover program) GBP structure, we obtain the theoretical

spectrum shown in Figure 7B (7A is the experimental spectrum, in the form of a stick diagram).

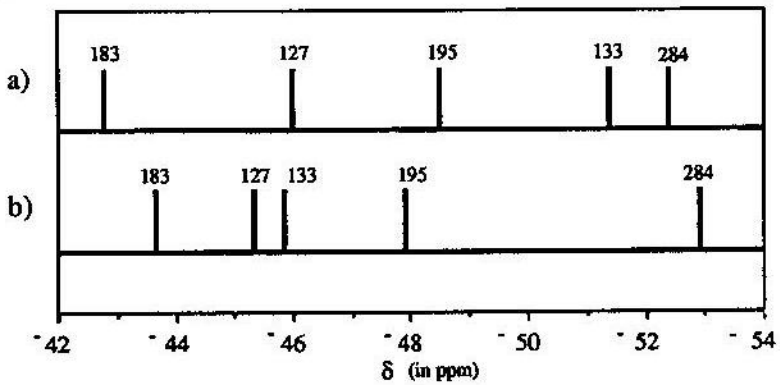

Figure 7. Uniform field point charge calculation of ^{19}F NMR spectrum for 5-F-Trp GBP. Calculation assumes AMBER charges on protein atoms, Ca(2+), STO-3G charges for glucose atoms, and a dielectric constant of 2.0. A 'random coil shift' of -47.6 ppm was determined by comparing the calculated and experimental spectra. Experimental spectrum based on Luck and Falke (1991; Ref. 4).

There is good general agreement between theory and experiment, for example, the overall range of shielding of ~9 ppm is in accord with the experimental range of 11 ppm, and four of the five resonances are in their correct sequence. However, the spectrum does vary considerably with minimization conditions (e.g. F charge, Ca^{2+} charge, number of steps) and it seems likely that molecular dynamics averaging over long trajectories will be required for more definitive calculations, as will the effects of field gradient (and possibly higher order) terms.

We now return to the topic of infra-red vibrational frequencies in proteins, and their electrical perturbation.

For about twenty-five years, it has been known that the infra-red vibrational frequencies of CO ligands *in a given protein* may vary, as a function of temperature, pressure, pH, and so forth. Given the ideas put forth above, we thought that these frequency shifts might be due to weak electrical interactions. Of particular importance here is the observation by Caughey (66) that there are always "four, and only four" ν_{CO} peaks, even when investigating over twenty protein systems.

It is clear from Figure 8 that four different electric fields can be generated in proteins containing distal histidine residues by the simple processes of $H^{\delta 1} \leftrightarrow H^{\varepsilon 2}$ tautomerism, combined with a 180° C^{β}-C^{γ} ring flip. The CO is close enough to be influenced by the histidines' dipole and quadrupole moments, so we carried out *ab initio* electronic structure calculations on the model system CO-methylimidazole, and found that at the four orientations shown in Figure 8, the field due to the quadrupole happens to be

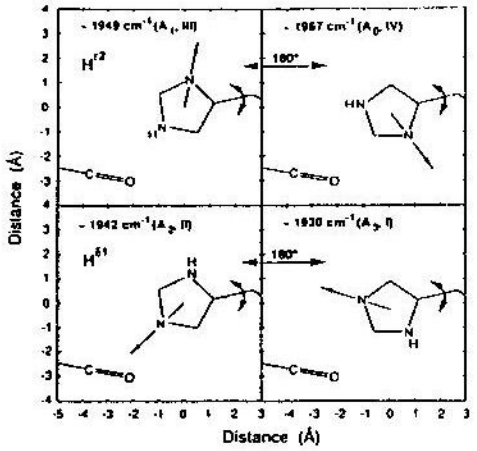

Figure 8. Schematic diagram illustrating the $H^{\delta 1}$ and $H^{\varepsilon 2}$ tautomers of the C^{β}-C^{γ} ring-flip isomers of the distal histidine in HbCO or MbCO, together with the FeCO fragment of the heme.

essentially proportional to the field due to the dipole (67). Thus, it is reasonable for a cosine dependence of just a dipole interaction to represent the deviation of the fundamental vibrational frequency, $\Delta\tilde{\nu}$, on θ, the angle between E_x and the CO bond axis. For simplicity, we write the fundamental vibrational frequency, $\tilde{\nu}$, in the carbonmonoxyhemeproteins as:

$$\tilde{\nu} = \tilde{\nu}_0 + a \cos\left[\frac{n360}{5} + b\right] \qquad (5)$$

where $\tilde{\nu}_0$ and a are variables that describe the field-free fundamental vibrational frequency and the histidines' local charge field, which based on dipole moment and other considerations is expected to be ~4 x 10^7 Vcm^{-1}. n takes the values -1,0, 1,2 by symmetry, and b reflects in a simple way the orientation of the CO bond axis with respect to the imidazole, as shown in Figure 8.

We obtain excellent agreement with the experimental observations on carbonmonoxyhemoglobin (HbCO) using the following parameters: $\tilde{\nu}_0$ = 1954 cm^{-1}, a = -23 cm^{-1}, b = -11° and these and other results are shown for several proteins graphically in Figure 9.

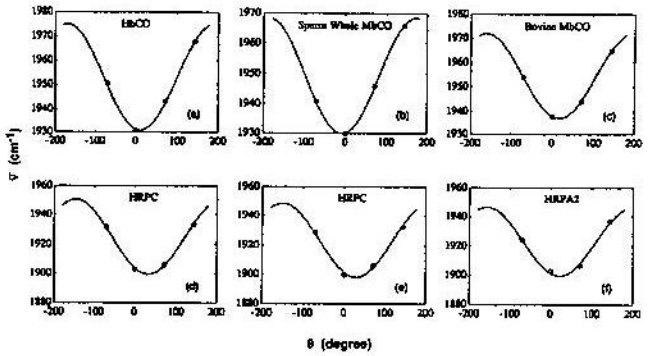

Figure 9. Comparison between experimental data (circles) and Eq. 5 (solid curve) for (a) HbCO; (b) sperm whale MbCO; (c) bovine heart MbCO; (d) horseradish peroxidase (mainly C isoenzyme); (e) horseradish peroxidase, C isoenzyme; and (f) horseradish peroxidase, A_2 isoenzyme.

Thus, the electric field generated by the distal histidine, which is immediately adjacent to the CO ligand, has four projections (cos -82°, cos -10°, cos 62°, cos 134°) due to the presence of a large dipole moment vector which rotates by 360/5 = 72° in the $H^{\delta 1}$ and $H^{\epsilon 2}$ tautomers of the two, 180° ring-flip isomers. The resultant fields are then ≈ 5.5 x 10^6 Vcm^{-1}, 3.9 x 10^7 Vcm^{-1}, 1.9 x 10^7 Vcm^{-1} and -2.8 x 10^7 Vcm^{-1}. Fields of this size significantly affect vibrational stretching frequencies. However, since we have used three adjustable parameters to fit four vibrational frequencies, the question of the adequacy of this fitting procedure needs to be addressed. Can we fit anything?

There are 4!/2=12 possible combinations of the four dipole moment vector orientations for the distal histidine residue. We have investigated several different proteins to determine whether all of these combinations can be fit by judicious choice of ν_0, a and b. For e.g. mouse HbCO, the 12 solutions yield the following r.m.s. deviations between theory and experiment: 0.1, 0.8, 3.2, 4.1, 4.1, 6.1, 6.9, 8.8, 8.9, 9.9, 10.7 and 11.8 cm^{-1}. Clearly, there are at most two solutions, having b = -11, -61°, and only the first one is close to that anticipated from x-ray studies of CO hemoglobins. Similar behavior is found for other proteins, so it appears that varying ν_0, a and b is only capable of producing a small number of acceptable solutions.

Electrostatic Effects on Quadrupole Coupling Constants

As mentioned in the previous section, in our recent work on CO-labelled heme proteins (61) we also found from the experimental results a correlation between the quadrupole coupling constants of the ^{17}O nucleus in CO and ν_{CO}. The experimental results, given in Fig. 10A, show an essentially linear correlation between the e^2qQ/h and ν_{CO}. We

calculated the electric field gradient experienced by ^{17}O from well correlated, ab initio wave functions using a large basis, and the effect of an external electric field of various strengths was explicitly included. The results are given on Fig. 10B. As for the chemical shifts, the relative changes due to application of a uniform electric field to CO are quite similar to those seen between CO experiencing the different environments of the various heme proteins. The correlation is well reproduced by these calculations; the slopes of the lines in Figs. 10A and 10B are 0.011 and 0.017 MHz/cm^{-1}, respectively.

We can extend that analysis and apply DHF to calculate the effects of external fields on the quadrupole coupling just as we have for the chemical shielding. In a series of papers (68-70), Sternheimer presented an analysis of the effect of an external point charge on the field gradient due to the electron distribution at a nucleus of an atom. The original analysis gives, in effect, the extent to which a nuclear quadrupole polarizes an isolated atom's electron distribution (68). Subsequently, it was shown that to second order it was equivalent to view the perturbation as either that of the nuclear quadrupole inducing a quadrupole moment in the atom's electrons, or an external charge inducing a field gradient at the nucleus. Simply, the field gradient at a nucleus is taken to be a "shielded" external field gradient:

$$V_{zz} = V_{zz}^{ext}(1 - \gamma) \qquad (6)$$

where γ is the shielding factor. In ^{83}Kr, for example, γ = –77.5±15 (71), according to a least squares fit of experimental values of V_{zz} vs. V_{zz}^{ext} for a number of Kr–X dimer

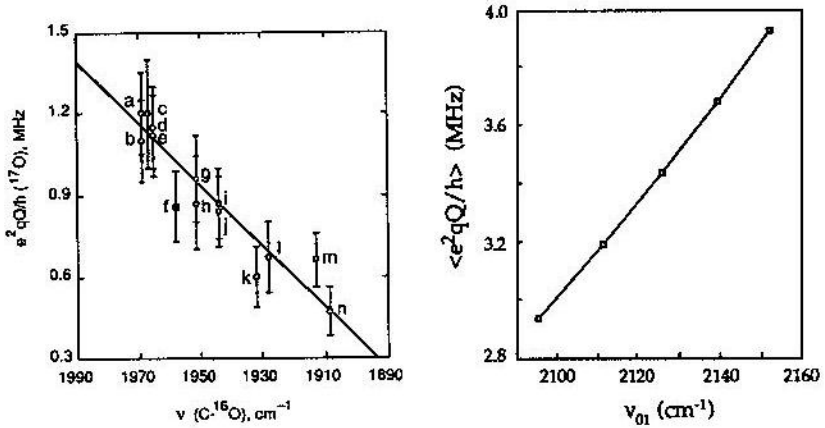

Figure 10. A.e^2q Q/h versus ν_{CO} for CO in heme proteins. B. $\langle e^2qQ/h \rangle$ for the ground vibrational state of CO (in MHz) calculated for different axial electric fields, versus the vibrational frequency shifts that are calculated to arise due to the fields. The upper rightmost point is the field-free data point. Note that ν_{CO} decreases from left to right in A while it increases in B.

complexes, where V_{zz} was found from the experimental χ value, and V_{zz}^{ext} was found from the low order electrical moments of the partner molecule.

The analysis was extended to ionic diatomic molecules (70) to include the added effect of the induced dipole moment. Buckingham (72) formally wrote out the expression to explicitly include the effects of uniform fields on ions, in effect by adding a term to Eqn. (6)

$$V_{zz} = V_{zz}^{ext}(1-\gamma)+\varepsilon V_z^2 \qquad (7)$$

where ε is the second order field gradient response due to the uniform field. Engström, et. al. (73) applied these ideas to covalent molecules, using a perturbation approach. Legon and Millen (74) have used this approach phenomenologically to experimentally determine for the first time the first order response of the field gradient due to an external electric field for HCl.

Table 3. Field Gradient and Field Gradient Polarizabilities of Several Small Molecules (a.u.)

Molecule		q^a	q_z	q_{zz}	q_{xx}	$q_{z,z}$	$q_{x,x}$	$q_{zz,zz}$	$q_{xx,xx}$
CH_3F	C	0.5947	4.649	-2.228	-2.049	-2.030	-13.65	-11.38	-21.19
	F	3.0950	-13.043	5.998	-0.797	70.216	-2.76	99.44	25.02
HF	F	2.9052	-8.569	10.448	-5.068	52.943	-37.17	73.03	-43.04
	H	0.5803	-0.745	0.856	0.214	2.716	0.55	1.93	0.05
HCCH	C	-0.3570	5.854	4.695	-1.955	-11.268	-27.23	33.95	-49.65
	H	0.3650	0.872	1.566	0.239	1.814	-0.14	7.41	-1.56
HCN	N	-1.1470	7.126	4.229	-1.966	10.249	-15.69	63.99	-29.44
	C	-0.4618	-5.364	4.555	-0.939	1.764	-11.28	46.46	-19.46
	H	0.3443	-0.767	1.467	0.271	1.930	0.58	8.04	0.24
CH_4	C	0.0	0.0	1.410	-0.705	19.482	-9.74	34.34	-17.17
	H	0.0	0.259	-0.077	0.039	-2.203	1.10	-4.81	2.40
H_2O	O	-1.8617	-2.155	6.794	-5.197	64.868	-52.69	94.83	-93.86
NH_3	N	-0.9665	0.161	9.728	-1.624	131.236	13.38	234.08	-5.86
CO	O	-0.6469	6.068	5.793	-3.289	-2.162	-7.44	-90.87	-17.44
	C	-1.1226	-2.603	1.541	1.209	22.923	11.66	62.11	14.28
HCl	Cl	3.6050	-17.399	23.877	-16.670	67.352	-135.24	229.33	-222.70
	H	0.3076	-0.748	0.919	0.259	2.252	0.32	3.16	-1.15

[a]Following convention, we use q to denote V_{zz}^{Nuc}, so that, e.g., $q_{x,yy} = \dfrac{\partial^2 V_{zz}^{Nuc}}{\partial V_x \partial V_{yy}}$.

Except for H_2O, the z-axis is the molecular symmetry axis. For H_2O, the z-axis is perpendicular to the molecular plane.

[b]This property is q_x. q_z is identically zero by symmetry.

With the analytical capability of DHF, we approach this problem head-on and calculate the derivatives of the field gradient at a nucleus with respect to the elements of the external electrical potential.

$$V_{zz}^{Nuc} = V_{zz,o}^{Nuc} + V_{zz,x}^{Nuc}V_x + V_{zz,y}^{Nuc}V_y + V_{zz,z}^{Nuc}V_z + \frac{1}{2}V_{zz,xx}^{Nuc}V_{xx}^2 + \ldots \qquad (8)$$

(V_{zz}^{Nuc} is the electric field gradient at the particular nucleus.) Both Bacskay, et al. (75,76) and Fowler (77) have presented a derivative approach to calculating certain of the terms in Eqn. (6). We can obtain all such values, and in Table 3 we present results for several small molecules. The results can be used to anticipate the effect on quadrupole coupling constants of the electrical influence of nearby molecules.

Summary

Overall, our results suggest the following:

1) For small isolated molecules, SCF level calculations (e.g. DHF) can give accurate representations of the chemical shielding tensors.

2) For larger molecules, long-range contributions to shielding in many instances contain calculable contributions from weak electrical interactions, which may be computed by using the multipole shielding polarizabilities such as we have obtained from DHF theory.

3) In CO heme proteins, there are strong correlations between $\delta_i(^{13}C)$, $\delta_i(^{17}O)$, $e^2qQ/h(^{17}O)$ and $\nu_{C\text{-}O}$, and these experimental trends are reproduced in DHF theory.

4) The four major conformational substates evidenced in the IR spectra of heme proteins are likely due to 180° ring flips about C^{β}-C^{γ} of the two imidazole tautomers.

5) For ^{19}F NMR of (labelled) proteins, weak electrical interactions describable by the dipole shielding polarizability and the uniform components of the field appear to make significant contributions to the observed spectral shifts.

6) For ^1H, ^{13}C, ^{17}O and ^{19}F NMR in proteins, there is a good correlation between known shielding ranges and $\bar{A}_x$, suggesting a range of uniform fields of ≈ 0.008 au, in basic agreement with fields calculated using a variety of electrostatic modelling approaches.

7) The range of fields in proteins as deduced from our NMR and IR results on a dozen heme proteins, from calculations on GBP, from the relation between $\bar{A}_x$ and the overall shielding ranges for several nuclei, and from electrostatics calculations by others, are all rather similar, and support the idea that both NMR and IR frequency shifts in proteins (and other macromolecules) will be influenced by such long range interactions.

Acknowledgements

This work was supported in part by the US National Institutes of Health (grants HL-19481 and GM-40426), the US National Science Foundation (grant CHE 9107317), and by the American Heart Association, with funds contributed by the AHA, Illinois Affiliate, Inc.

J. Pearson is a National Institutes of Health Postdoctoral Fellow (grant GM-14545).

References

1. Bax, A., Ikura, M., Kay, L., Torchia, D.A., and Tschudin, R. (1991) J. Magn. Reson. 86, 304; Clone, G. M. and Groenenborn, A. M. Progr. NMR Spectroscopy 23, 43-92 .
2. McDonald, C. C. and Phillips, W. D. (1969) J. Amer. Chem. Soc. 91, 1513.
3. Allerhand, A., Childers, R. F., and Oldfield, E. (1973) Biochemistry 12, 1335; Sykes, B. D. and Weiner, J. H. (1980) Magn. Res. Biol. 1, 171.
4. Gerig, J. T. (1989) Meth. Enzym. 177, 3.
5. Millett, F. and Raftery, M. A. (1972) Biochem. Biophys. Res. Commun. 47, 625.
6. Luck, L. A. and Falke, J. J. (1991) Biochemistry 30, 4248.
7. Glushka, J., Lee, M., Coffin, S., and Cowburn, D. (1989) J. Am. Chem. Soc. 111, 7716.
8. Park, K. D., Guo, K., Adebodun, F., Chiu, M. L., Sligar, S. G., and Oldfield, E. (1991) Biochemistry 30, 2333.
9. Oldfield, E., Montez, B., Patterson, J., Harrell, S., Lian, C., and Le, H., unpublished results.
10. Hoch, J. C., Ph.D. Thesis (1983) Harvard University, University Microfilms International, Ann Arbor, MI, #8322365.
11. Pardi, A., Wagner, G., and Wüthrich, K. (1983) Eur. J. Biochem. 137, 445.
12. Redfield, C. and Dobson, C. M. (1990) Biochemistry 29, 7201.
13. Oldfield, E. Abstracts, American Chemical Society Southeastern-Southwestern Meeting, New Orleans, LA, December 7, 1990.
14. Williamson, M. P. and Asakura, T. (1991) J. Magn. Res. 94, 557.
15. Williamson, M. P., Asakura, T., Nakamura, E., and Demura, M. J. Biomol. NMR, in press.
16. Asakura, T., Nakamura, E., Asakawa, H., and Demura, M. (1991) J. Magn. Res. 93, 355.
17. Wagner, G., Pardi, A., and Wüthrich, K. (1983) J. Am. Chem. Soc. 105, 5948.
18. Ösapay, K. and Case, D. A. (1991) J. Am. Chem. Soc. 113, 9436.
19. Dalgarno, D. C., Levine, B. A., and Williams, R. J. P. *Bioscience Reports*, **3**, 443 (1983); A. Pastore and V. Saudek, *J. Magn. Res.*, **90**, 165 (1990); M. P. Williamson, *Biopolymers*, **29**, 1423 (1990); I. D. Kuntz, P. A. Kosen and E. C. Craig, *J. Am. Chem. Soc.*, **113**, 1406 (1991).
20. Wishart, D. S., Sykes, B. D., and Richards, F. M. (1991) J. Mol. Biol. 222, 311.
21. Wishart, D. S., Sykes, B. D., and Richards, F. M. (1992) Biochemistry 31, 1647.
22. Buckingham, A. D. (1960) Can. J. Chem. 38, 300.
23. Batchelor, J. G. (1975) J. Am. Chem. Soc. 97, 3410.
24. Pera, S. and Bax, A. (1991) J. Am. Chem. Soc. 113, 5490.
25. Bartlett, R. J. and Brandas, E. J. (1972) J. Chem. Phys. 56, 5467; Bartlett, R. J. and Shavitt, I. (1977) Chem. Phys. Lett. 50, 190.
26. McWeeny, R. (1961) Phys. Rev. 126, 1028.
27. Stevens, R. M., Pitzer, R. M. and Lipscomb, W. N. (1963) J. Chem. Phys. 38, 550.
28. Gerratt, J. and Mills, I. M. (1968) J. Chem. Phys. 49, 1719.
29. Pulay, P. (1969) Molec. Phys. 17, 197.
30. Dykstra, C. E. and Jasien, P. G. (1984) Chem. Phys. Lett. 109, 388.
31. Augspurger, J. D. and Dykstra, C. E. (1991) J. Phys. Chem. 95, 9230.
32. Augspurger, J. D. and Dykstra, C. E. (1990) J. Comp. Chem. 11, 105.

33. Augspurger, J. D., Bernholdt, D. E., and Dykstra, C. E. (1990) J. Comp. Chem. 11, 972.
34. Chan, S. I. and Das, T. P. (1962) J. Chem. Phys. 37, 1527.
35. Ditchfield, R. (1972) J. Chem. Phys. 56, 5688.
36. Ditchfield, R. (1974) Mol. Phys. 27, 789.
37. Epstein, S. T. (1973) J. Chem. Phys. 58, 1592.
38. Sadlej, A. J. (1975) Chem. Phys. Lett. 36, 129.
39. Yaris, R. (1976) Chem. Phys. Lett. 38, 460.
40. Kutzelnigg, W. (1980) Isr. J. Chem. 19, 193.
41. Schindler, M. and Kutzelnigg, W. (1982) J. Chem. Phys. 76, 1919.
42. Hansen, A. E. and Bouman, T. D. (1985) J. Chem. Phys. 82, 5035; (1989) 91, 3552.
43. Stephens, P. J., Jalkanen, K. J., Lazzeretti, P., and Zanasi, R. (1989) Chem. Phys. Lett. 156, 509.
44. Stephens, P. J. and Jalkanen, K. J. (1989) J. Chem. Phys. 91, 1379.
45. Lazzeretti, P., Malagoli, M., and Zanasi, R. (1991) Chem. Phys. 150, 173.
46. Geertsen, J. (1989) J. Chem. Phys. 90, 4892.
47. Oddershede, J. and Geertsen, J. (1990) J. Chem. Phys. 92, 6036.
48. Wolinsky, K., Hinton, J. F., and Pulay, P. (1990) J. Am. Chem. Soc. 112, 8251.
49. Hinton, J. F., Guthrie, P., Pulay, P., and Wolinski, K. (1992) J. Am. Chem. Soc. 114, 1604.
50. Day, B. and Buckingham, A. D. (1976) Mol. Phys. 32, 343.
51. Lazzeretti, P., Zanasi, R., and Cadioli, B. (1977) J. Chem. Phys. 67, 382.
52. Lazzeretti, P. and Zanasi, R. (1977) Int. J. Quan. Chem. 12, 93; (1978) J. Chem. Phys. 68, 1523.
53. Chesnut, D. B. and Foley, C. K. (1985) Chem. Phys. Lett. 118, 316.
54. Chesnut, D. B. and Foley, C. K. (1986) J. Chem. Phys. 85, 2814.
55. Chesnut, D. B. and Moore, K. D. (1989) J. Comp. Chem. 10, 648.
56. Augspurger, J. D. and Dykstra, C. E. (1991) Chem. Phys. Lett. 183, 410.
57. Dunning, T. H. (1970) J. Chem. Phys. 53, 2823; (1971) 55, 716.
58. Huzinaga, S. (1965) J. Chem. Phys. 42, 1293.
59. Dykstra, C. E., Liu, S.-Y., and Malik, D. J. (1989) Adv. Chem. Phys. 75, 37.
60. Note that the convention of Eqn. 3 corresponds to a diamagnetic susceptibility being positive.
61. Augspurger, J. D., Dykstra, C. E., and Oldfield, E. (1991) J. Am. Chem. Soc. 113, 2447.
62. Dykstra, C. E. (1989) J. Am. Chem. Soc. 111, 6168.
63. Dykstra, C. E. (1987) J. Phys. Chem. 91, 6216.
64. Gutowsky, H. S., Germann, T. C., Augspurger, J. D., and Dykstra, C. E. (1992) J. Chem. Phys. 96, 5808.
65. Dao-Ping, S., Lao, D.-I., and Remington, S. J. (1989) Proc. Natl. Acad. Sci. USA 86, 5361; Hol, W. G. J. (1985) Prog. Biophys. Molec. Biol. 45, 149; Sharp, K. A. and Honig, B. (1990) Ann. Rev. Biophsy. Chem. 19, 301; Warshel, A. and Åqvist, J. (1991) Annu. Rev. Biophys. Biophys. Chem. 20, 267; Lee, F. S. and Warshel, A. submitted to J. Chem. Phys.
66. Potter, W. T., Hazzard, J. H., Choe, M. G., Tucker, M. P., and Caughey, W. S. (1990) Biochemistry 29, 6283.
67. Oldfield, E., Guo, K., Augspurger, J. D., and Dykstra, C. E. (1991) J. Am. Chem. Soc. 113, 7537.

68. Sternheimer, R. (1950) Phys. Rev. 80, 102; (1951) 84, 244; (1952) 86, 316; (1954) 95, 736; (1956) 102, 731; (1966) 146, 140.
69. Sternheimer, R. M. and Foley, H. M. (1953) Phys. Rev. 92, 1460.
70. Foley, H. M., Sternheimer, R. M., and Tycko, D. (1954) Phys. Rev. 93, 734.
71. Campbell, E. J., Buxton, L. W., Keenan, M. R., and Flygare, W. H. (1981) Phys. Rev. A24, 812.
72. Buckingham, A. D. (1962) Trans. Farad. Soc. 58, 1277.
73. Engström, S., Wennerström, H., Jönsson, B., and Karlström, G. (1977) Mol. Phys. 34, 813.
74. Legon, A. C. and Millen, J. D. (1988) Chem. Phys. Lett. 144, 136; (1988) Proc. Roy. Soc. A 417, 21.
75. Bacskay, G. and Gready, J. E. (1988) J. Chem. Phys. 88, 2526.
76. Bacskay, G., Kerdraon, D. I., and Hush, N. S. (1990) Chem. Phys. 144, 53.
77. Fowler, P. W. (1989) Chem. Phys. Lett. 156, 494; (1990) Chem. Phys. 143, 447.